Conformation of Poly(methacrylic acid) Chains in Dilute Aqueous Solution

Lorena Ruiz-Pérez,[†,⊥] Andrew Pryke,[‡] Michael Sommer,[†,§,#] Giuseppe Battaglia,[‡,&] Ian Soutar,[‡,||] Linda Swanson,[*,‡] and Mark Geoghegan[†]

Department of Physics and Astronomy, University of Sheffield, Hicks Building, Hounsfield Road, Sheffield S3 7RH, UK; Department of Chemistry, University of Sheffield, Brook Hill, Sheffield S3 7HF, UK; and Lehrstuhl für Physikalische Chemie II, Universität Bayreuth, D-95440 Bayreuth, Germany

Received May 1, 2007; Revised Manuscript Received December 31, 2007

ABSTRACT: Poly(methacrylic acid) (PMAA) undergoes a conformational transition between pH 4 and 6 from a hypercoiled structure to a water-swollen state. There has been much speculation as to the exact nature and driving force of the transition. In this paper, we present a comprehensive investigation of the conformational switch of PMAA using techniques which report on various length scales: fluorescence energy transfer experiments provide unique information on the nanometer length scale while dynamic light scattering (DLS) offers an insight into longer range interactions involved in the transition. Fluorescence energy transfer measurements demonstrate that PMAA undergoes subtle molecular rearrangements between pH 2 and 5 as short-range hydrophobic interactions between methyl groups are broken down by increasing concentrations of mutually repulsive carboxylate anions. Although such rearrangements have been proposed to account for the pH behavior of PMAA, we reveal them experimentally using techniques sensitive to nanoscale events. Fluorescence lifetime measurements indicate a rather complex structure within the collapsed chain, and time-resolved anisotropy measurements also demonstrate the importance of intramolecular interactions at low pH. A critical point, at pH 5.7, is reached in terms of the carboxylate anion concentration where a macroscopic transition occurs (as monitored by DLS): the concentration of carboxylate anions is such that repulsive interactions dominate, and a switch occurs from a compact, globular form to an expanded state when neutralization of the PMAA is complete. We conclude that small-scale rearrangements in structure occur between pH 2 and 5, rather than a large-scale expansion, which is then followed by a macroscopic change in dimension at the neutralization point. Our results comprehensively describe the conformational behavior of PMAA and reconcile, to some extent, previous conflicting experimental data in the literature.

Introduction

The behavior of polyelectrolytes in solution remains an active area of research because of the ability to control their behavior in response to different external stimuli as well as recognition of the importance of water-soluble polymers. The magnitude, extent, and range over which conformational changes may occur have many possible applications. These extend from semiconductor devices, molecular sensors, nanoscale pumping devices, controlled wetting, new optics, microelectronics, drug delivery, flocculants, and super-absorbants.[1] Such knowledge may also assist in elucidating the roles that complex biological polyelectrolytes such as DNA play in biochemical processes.[2,3]

Poly(methacrylic acid) (PMAA), a weak polyacid, is of particular interest because it exhibits a marked pH-induced conformational transition. This transition has been studied by different techniques including potentiometric titration,[4−8] viscosimetry measurements,[9−12] solubilization of hydrophobic molecules in aqueous PMAA,[13−19] calorimetry,[18,20−22] Raman spectroscopy,[23] and scattering methods.[24−29] The results obtained from these different techniques have indicated that at pH 4 PMAA exists in a hypercoiled conformation with most of the methyl groups located in the interior of the coil due to hydrophobic interactions. At pH 6, the chain expands to a more open water-swollen structure due to Coulombic repulsions between carboxylate groups. However, the exact nature of the switch in conformation remains unresolved. Some studies[8,9] suggest that the change is cooperative and occurs in one step, analogous to the helix−coil transition of polypeptides.[30] Contrary to this assumption, data from Raman spectroscopy indicate the presence of a multiplicity of structures, which suggests that the transition occurs as a progressive rather than a cooperative change.[23]

Techniques with resolution in a range from 0.2 to 10 nm are needed to observe the transition on the level of single molecules. Fluorescence spectroscopic measurements offer such resolution, and also allow in-situ monitoring of processes which occur within the polymer chains when the pH is changed. In order to follow such processes, it is necessary to attach a small amount of fluorescent dye to the polymer under study. These chromophores can be introduced as either a dispersed molecular probe or a covalently bound label. Different probes have been used in order to study the conformational transition of PMAA: for example, pyrene has been used to investigate the kinetics of coil expansion,[16,18,31] and the existence of structural microdomains,[16,31,32] within the hypercoiled conformation at low pH. Other fluorescence reporters used to study PMAA include solubilized probes such as coumarin[33] or covalently bound labels

* Corresponding author. E-mail: l.swanson@sheffield.ac.uk.
† Department of Physics and Astronomy, University of Sheffield.
‡ Department of Chemistry, University of Sheffield.
§ Universität Bayreuth.
|| Deceased.
⊥ Present address: Department of Chemistry, University of Sheffield, Brook Hill, Sheffield S3 7HF, UK.
Present address: Lehrstuhl für Makromolekulare Chemie I, Universität Bayreuth, D-95440 Bayreuth, Germany.
& Present address: Department of Engineering Materials, Kroto Research Institute, North Campus, University of Sheffield, Broad Lane, Sheffield S3 7HQ, UK.

10.1021/ma0709957 CCC: $40.75
Published on Web 02/27/2008

such as dansyl,[15] diphenylanthracene,[34] and 1-vinylnaphthalene.[35]

The combination of two chromophores in polymeric systems is a commonly used procedure to investigate molecular distances. For this purpose, nonradiative energy transfer (NRET) measurements are performed in donor−acceptor labeled polymers. NRET depends on the relative orientation and separation distance, *R*, between the donor−acceptor pairs, which can be located on the same polymer (as in the present study) or on different polymers in a blend.[36] Since the chromophores are attached to the polymer chains, changes in chain conformation result in changes in the separation distance between the donor−acceptor dyes.[37,38] The variation in distance is monitored as a greater or lower efficiency in energy transfer from the donor to the acceptor. For this reason NRET is commonly called the "spectroscopic ruler" technique.[39−41]

One of the most popular combinations of chromophores used for NRET measurements is with a naphthalene donor and an anthracene acceptor. This particular pair has some advantages: there is a range of wavelengths (290−310 nm) where naphthalene can be excited with minimal direct excitation of anthracene, naphthalene monomer and anthracene fluorescence bands are quite different and easy to distinguish, and the anthracene chromophore can be covalently bound to polymers containing naphthalene in different ways.[42]

In the present study we have used acenaphthylene (ACE) and anthrylmethyl methacrylate (AMMA) labels covalently attached to the PMAA backbone where the chromophores are randomly distributed along the chain. Energy transfer measurements were performed on the donor (ACE)−acceptor (AMMA) pair using steady-state fluorescence intensity and emission decay experiments as a function of pH. In addition to these techniques, we have also employed time-resolved anisotropy measurements (TRAMS) by selective excitation and analysis of the AMMA label in order to provide supplementary information on the segmental dynamics of PMAA in aqueous solution.

Although other authors have studied PMAA containing naphthyl and/or anthryl labels, previous work has concentrated on the combination of two techniques: steady state and lifetime measurements[34,43,44] or time-resolved anisotropy measurements (TRAMS) and lifetime measurements in the case of single-labeled naphthyl-PMAA.[35,45] We report here on a complete characterization of the pH-dependent conformational change which occurs in PMAA in dilute solution using a combination of three fluorescence techniques: energy transfer, fluorescence lifetime, and TRAMS. In addition to these fluorescence experiments, complementary data on the conformational switch of PMAA were obtained from dynamic light scattering (DLS) measurements. This latter technique allows estimation of the polymer chain dimensions at different degrees of ionization.

Experimental Section

Polymer Synthesis. Polymerization of methacrylic acid (MAA) and copolymerization of MAA with the comonomer labels ACE and AMMA were performed by free radical polymerization. The ACE monomer was added at 0.5 mol % into the initial feed for single-labeled polymers; for double-labeled samples, the loading was 0.5 mol % ACE and 1.5 mol % AMMA. (Since dye labels are hydrophobic, and can be used as "hydrophobic modifiers" of polyelectrolytes,[46,47] it is necessary to keep their concentration low to be confident that their effect is limited to acting as fluorescence labels and that no perturbation of the polymer behavior results.) The polymerization was performed in benzene using azobis(isobutyronitrile) as the initiator.

The samples were thoroughly degassed, by repeated freeze pump−thaw cycles, sealed under high vacuum ($\sim 10^{-4}$ mbar), and polymerized at 60 °C for 48 h. In order to ensure an even distribution of fluorescent chromophores along the polymer chain most samples were allowed to proceed to only 10−20% conversion. The polymers were purified by multiple dissolution (five times) into methanol followed by precipitation into diethyl ether. This preparation produced a polymer (ACE−PMAA) bearing a naphthyl chromophore rigidly bound to the chain backbone through two single covalent bonds (which prevent label motion independent of the polymer segment to which it is bound). A second, double-labeled, sample (ACE−AMMA−PMAA) containing ACE and an anthryl chromophore bound via a methacrylate group (AMMA) was also prepared by this general method.

Sample Characterization. Molecular weights of the labeled PMAA were measured by gel permeation chromatography using a HP 1047A refractive index detector. Molecular weights based on poly(ethylene oxide) standards were 72 and 80 kg mol^{-1} for the single-labeled (ACE−PMAA) and double-labeled sample (ACE−AMMA−PMAA), respectively. Polydispersities were 2.9 and 2.7 for ACE−PMAA and ACE−AMMA−PMAA, respectively.

To calculate the amount of label in the polymer,[48] the PMAA was dissolved at 0.01 wt % in spectroscopic grade methanol, and UV spectra were recorded with a Hitachi U-2010 spectrometer, scanning from 200 to 500 nm. For ACE−AMMA−PMAA the anthryl content was calculated prior to estimation of the naphthyl loading. Correction was then made for the small amount of AMMA absorption at 290 nm to allow the ACE content to be determined. For ACE−AMMA−PMAA the naphthyl and anthryl contents were 0.56 and 0.23 mol %, respectively, (i.e., one ACE per 221 MAA monomers and one AMMA per 440 MAA monomers). For ACE−PMAA, UV absorption revealed 0.82 mol % of chromophore (one ACE for 130 units of MAA).

Instrumentation and Analysis. Steady state measurements were performed using a LS-50B Perkin-Elmer luminescence spectrometer equipped with a Xe discharge lamp pulsed for 8 μs at 20 kW (fwhm for the pulse was better than 10 μs). Data analysis was performed using Perkin-Elmer Fluorescence Data Manager software (FL WinLab). PMAA was dissolved in water at 0.01 wt %, which is dilute enough to observe isolated macromolecule behavior. (The chain overlap concentration would be expected to be ~100 times this value.) Both single- and double-labeled samples were excited at 290 nm, the maximum excitation wavelength of ACE. Emission intensity was recorded between 310 and 500 nm, which included fluorescence from naphthalene (340 nm) and anthracene (420 nm).

The degree of energy transfer was monitored by calculation of the ratio of the emission intensities of AMMA at 420 nm to that of ACE at 340 nm (I_A/I_N). The data were obtained using the steady-state fluorimeter combined with a flow cell and peristaltic pump system, such that liquid from a stirred vessel (the pH of which was accurately adjusted by means of a burette containing acid or base) was constantly circulated through the flow cell. Aliquots of 0.5 M HCl or 1.0 M NaOH were added to the solution to change the pH, which was recorded as soon as the solution stabilized.

Fluorescence lifetime measurements were carried out on a single photon counting spectrometer equipped with an IBH System 5000 coaxial nanosecond flash lamp and a photomultiplier connected to a time-to-amplitude converter (TAC) and multichannel analyzer (MCA) which allows fluorescence decays in the range of 0.7 ns to ~0.2 μs to be studied. A combination of filters to remove the stray excitation associated with the instrument response function allows fluorescence lifetime measurements as short as 0.7 ns. All fluorescence decays for the luminescently labeled samples were collected at the "magic angle" of 54.7° with respect to that of the vertically polarized excitation. Excitation and emission wavelengths of 290 and 340 nm, respectively, were employed in the study of both ACE−PMAA and ACE−AMMA−PMAA. Data were fitted using the IBH software to simple exponentials. The decays were (least-square) fitted to a sum of exponentials

$$I = \sum_i^n A_i \exp\left(\frac{-t}{\tau_i}\right) \quad (1)$$

where the terms A_i are constants and τ_i are fluorescence lifetimes (t is time). In the present study, $n = 2$ or 3, depending on the complexity of decays. (A single-exponential fit was never judged statistically sufficient to obtain a good fit to our data.)

The average lifetime $\langle\tau\rangle$ not only provides information on the conformational transition but also is needed to calculate the efficiency of energy transfer. $\langle\tau\rangle$ is calculated using

$$\langle\tau\rangle = \frac{\sum_i A_i \tau_i^2}{\sum_i A_i \tau_i} \tag{2}$$

Time-resolved anisotropy measurements (TRAMS) were performed on an Edinburgh Instruments 199 fluorescence time-correlated single photon counter modified with a computer-controlled toggling polarizer accessory. The excitation source used was an IBH Nanoled operating at a repetition rate of 1 MHz and a wavelength of 370 nm. The emission wavelength (450 nm) was isolated using an interference filter. (This experimental setup allows selective excitation and analysis of the AMMA fluorescence.)

In the TRAMS experiment, vertically polarized radiation is used to photoselect (via absorption) those chromophores whose transition vectors (dipole moments) lie in a parallel plane to the polarization of the incident radiation. If the luminescent molecule remains stationary during its excited-state lifetime, the resultant radiation remains highly polarized, characteristic of the intrinsic anisotropy of that particular species. Light emitted from the molecules which change their orientation while excited will be polarized differently to the excitation radiation. Information regarding molecular motion is contained within the relative time-dependent intensities of luminescence observed in parallel [$I_{||}(t)$] and perpendicular [$I_{\perp}(t)$] planes to that of photoselection. The anisotropy function $r(t)$ can subsequently be derived from

$$r(t) = \frac{I_{||}(t) - I_{\perp}(t)}{I_{||}(t) + 2I_{\perp}(t)} \tag{3}$$

and is a useful means of deriving the relaxation information contained within the TRAMS experiment. Using eq 3, anisotropy decays of ACE−AMMA−PMAA were collected as a function of pH. Different procedures of analysis have been discussed elsewhere.[45] In the present studies, the raw anisotropy data $r(t)$ were directly fitted to a function (without any deconvolution with the experimental response function) which is assumed to model the decay of true anisotropy data. Assuming the dyes behave like an isotropic rotor in a fluid environment, the anisotropy can be modeled with

$$r(t) = r_0 \exp\left(\frac{-t}{\tau_c}\right) \tag{4}$$

where r_0 is the intrinsic anisotropy for the individual chromophores (constant for a particular fit) and τ_c is the correlation time, which is a measure of molecular motion.

For dynamic light scattering (DLS), it is important to increase the concentration of PMAA in order to increase the signal intensity.[49,50] Too large an increase in concentration results in aggregation, which can be detected by a *slow mode* (interchain effects) in the DLS experiments. This slow mode can be inhibited by adding salt to shield the charges. However, too much salt will affect the conformational transition. The best compromise between shielding interchain forces and maximizing intrachain forces was found at a concentration of 0.1 wt % of polymer and 0.01 M NaCl. Solutions were prepared by dissolving the same double-labeled PMAA used in fluorescence analysis in filtered 0.01 M NaCl water solution. The pH was adjusted by adding 0.5 M HCl and 1 M NaOH. Samples were prepared at least 16 h prior to the experiment in order to ensure that complete dissolution of the polymer had occurred and to equilibrate the pH, which was measured using a pH meter under constant stirring. To ensure that the samples were completely dust-free, solutions and samples were prepared in a clean room environment.

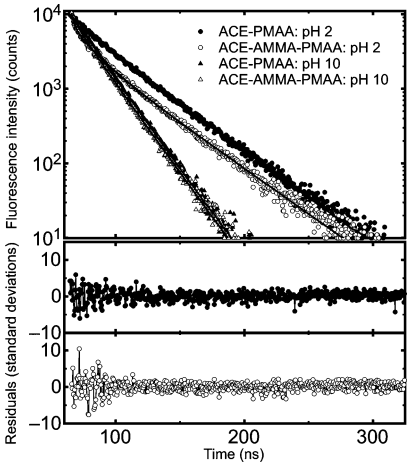

Figure 1. Fluorescence decays for ACE−AMMA−PMMA and ACE−PMAA respectively in acidic and basic conditions ($\lambda_{ex} = 290$ nm and $\lambda_{em} = 340$ nm). The residuals to the best fits for the pH 2 data are shown for the ACE−PMAA above and the ACE−AMMA−PMAA below. The deviation of the ACE−AMMA−PMAA with respect to ACE−PMAA at pH 2 is clearly visible. An extra lifetime component is needed to model the decay of the ACE−AMMA−PMAA fluorescence, which can be attributed to energy transfer from ACE to AMMA.

A BI-200 SM goniometer with 0.01° steps from Brookhaven Instruments Corp. was used. The excitation source was a He−Ne laser (with wavelength $\lambda = 633$ nm and maximum power output of 75 mW). Each solution (i.e., at different values of pH) was measured at angles of 40°, 60°, 90°, and 120°. The pinhole in front of the detector was set at 400 μm. The data collection time was 5 min for each experiment with a time window from 100 ns to 100 ms. The measured correlation functions were analyzed using cumulant analysis by polynomial fit. The linear relaxation rate $\Gamma = 1/\tau_d$ (where τ_d is a time constant representing the temporal decay in light scattering intensity fluctuation) was plotted as a function of the squared scattering vector (q^2) with the linear fit to the data forced through the origin (see Supporting Information), yielding the diffusion coefficient D_t as the slope ($\Gamma = D_t q^2$). The hydrodynamic radius R_H was determined using the Stokes−Einstein relation

$$R_H = \frac{k_B T}{6\eta D_t} \tag{5}$$

where k_B is the Boltzmann constant, T is the absolute temperature, and η is the solution viscosity.

Results and Discussion

Fluorescence Lifetime Measurements. In Figure 1, we show decay data for ACE emission at 340 nm from ACE−AMMA−PMAA and ACE−PMAA at pH 2 and pH 10. From the data it is evident that at high pH the ACE decay is independent of whether or not the AMMA acceptor is present. In acidic conditions, the duration of the decay increases due to hydrophobic forces of attraction which cause the chain to collapse, resulting in a more protective environment for the ACE label. It is worth noting that at low pH the donor decay of ACE−AMMA−PMAA deviates away from that of ACE−PMAA, indicating that energy transfer from ACE to AMMA occurs prior to any solvent quenching. This energy transfer adds complexity to the fluorescence decay of ACE−AMMA−PMAA: three exponential terms were required to fit the data adequately rather than the two components necessary in the absence of the anthryl label. This complexity is a consequence of a distribution of distances between different donor−acceptor pairs. At high pH,

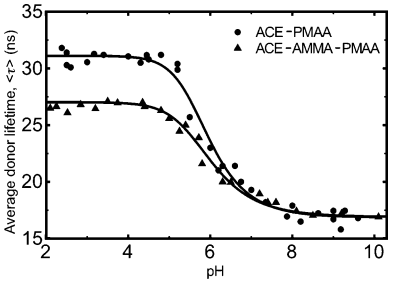

Figure 2. Average donor lifetime $\langle\tau\rangle$ for ACE−AMMA−PMAA and ACE−PMAA as a function of pH ($\lambda_{ex} = 290$ nm and $\lambda_{em} = 340$ nm). The solid lines are fits (using eq 6) to the data. The neutralization point calculated from these data is at a pH of 5.8 for the double-labeled polymer and 5.7 for the single-labeled polymer.

the chromophores move apart, and the fluorescence decay can be fitted to a dual-exponential model. The transient fluorescence of ACE−PMAA requires a double-exponential function to fit the data over the entire pH range. The quality of the fits to the ACE−AMMA−PMAA decay data is good with a normalized χ^2 given by $1.2 < \chi^2 < 1.6$. Those for the single-labeled polymer are even better with $1.0 < \chi^2 < 1.5$. Because these lifetime data at low pH are key to our understanding of the behavior of PMAA, we also show the residuals to the fits in Figure 1, which show these fits are appropriate on statistical grounds for the data presented.

The average lifetime, $\langle\tau\rangle$ analyzing the ACE emission at 340 nm, was calculated using eq 2 for both the single- and double-labeled polymers at various pH values. The $\langle\tau\rangle$ data are plotted as a function of pH in Figure 2. We note that between pH 2 and 5 $\langle\tau\rangle$ for ACE−PMAA is longer than that of ACE−AMMA−PMAA by ∼5 ns. This provides evidence for quenching due to energy transfer under these conditions.

At high pH (above the neutralization point), there is no significant difference in average lifetime between the samples due to energy transfer being inhibited by the extended conformation of the swollen chain (discussed below). In order to obtain the neutralization point, we fitted the data using a Levenberg−Marquardt routine to an empirical function

$$f(\mathrm{pH}) = h_2 + \frac{1}{2}(h_1 - h_2)\sqrt{\left(1 + \tanh\left(\frac{\Delta_1 - \mathrm{pH}}{\sigma_1}\right)\right)\left(1 + \tanh\left(\frac{\Delta_2 - \mathrm{pH}}{\sigma_2}\right)\right)} \quad (6)$$

which models the data very well. In eq 6, all parameters (h_1, h_2, Δ_1, Δ_2, σ_1, and σ_2) are fitted. Although this function is wholly empirical (h_1, h_2, Δ_1, Δ_2, σ_1, and σ_2 are introduced solely to fit the data and convey no physical meaning), it allows a mathematically accurate and rigorous means of calculating the neutralization pH. The neutralization point is obtained by setting $\partial^2 f/\partial(\mathrm{pH})^2 = 0$. The inflection point is located at a pH of 5.8 for ACE−AMMA−PMAA and 5.7 for ACE−PMAA.

Up to three different values of τ_i were required to fit the donor decay of ACE−AMMA−PMAA, which suggests that a rather more complex structure exists for this sample than usually presumed for PMAA. Different lifetimes correspond to different microenvironments with different degrees of hydrophobicity and/or viscosity.[15,18] The fractional contribution of the different lifetime components ($A_i/\sum_i A_i$) used to fit the naphthyl fluorescence decays in ACE−AMMA−PMAA is shown in Figure 3.

Previous work aimed at understanding the conformational structure of PMAA includes time-resolved anisotropy measurements on PMAA labeled with terminal dimethylanthracene.[51]

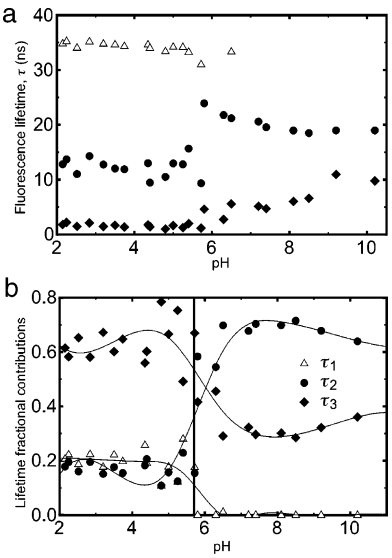

Figure 3. pH dependence of the three lifetimes (a) and their fractional contributions (b) used to fit the decays for ACE−AMMA−PMAA analyzing the ACE emission. The thick vertical line in (b) refers to the neutralization pH, and the solid lines are spline fits to guide the eye.

Here, the authors suggest that the polyelectrolyte can adopt a *pearl necklace* conformation at pH values below the neutralization point. The different lifetimes would then correspond to chromophores trapped either in the clusters (longer τ_i) or in the more open segments (shorter τ_i). However, in our work the labeled PMAA is of a relatively low molecular weight and so is incapable of forming such structures.[24]

We suggest that in acidic conditions the polyelectrolyte forms a coil with different levels of exposure to the solvent, which we refer to as a "layered onion" model. The most hydrophobic regions exist in a nucleus which is reflected by a contribution of 20% from the longest-lived component. Interactions between methyl groups are responsible for this compact structure. Presumably there are only traces of solvent present in the nucleus. Donor chromophores tightly trapped in this rigid pocket do not exhibit significant freedom of movement, and as a result their decays have a long lifetime of $\tau_1 \approx 34$ ns. Surrounding the nucleus is a region, affecting ∼20% of the chromophores, that is less tightly bound and contains slightly more solvent. Here the longer lifetime, which is in the range $10\text{ ns} < \tau_2 < 15$ ns, implies that there is more freedom of movement, afforded by the presence of water molecules for labels under these conditions. The shortest lifetime component ($\tau_3 < 5$ ns) most likely represents the outermost part of the chain, which accounts for 60% of the chromophores. It is possible that the shortest lifetimes are due to chains labeled at their ends, but given that the reaction was allowed to proceed to no more than 20% conversion, it is unlikely that these species would contribute to 60% of the decays. Although the current lifetime data suggest that there are three distinct regions of chain conformation, we did not fit the data to four or more lifetimes, which would have also provided reasonable results. (A triple-exponential function was deemed adequate by consideration of the statistical criteria used to judge the quality of fit.) Our results do not prove that these lifetimes represent a discrete core−shell−shell structure; it is likely that a gradual distribution of solvent composition exists. Similarly, our data do not prove that the nucleus contains the most collapsed part of the chains, and nor can we say that there is only one such "nucleus". Another possibility is the existence of domains giving rise to τ_2. In this respect, we believe that the layered "onion" model may be compared with a "plum

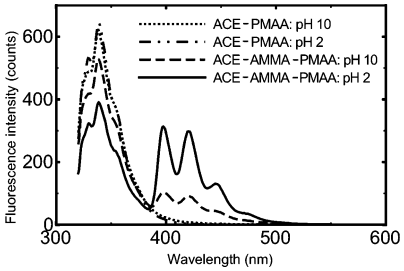

Figure 4. Steady-state spectra of both ACE−PMAA and ACE−AMMA−PMAA in aqueous solution (10^{-2} wt %) at different pH values. The emission wavelength λ_{em} is scanned from 310 to 550 nm, for a fixed excitation wavelength $\lambda_{ex} = 290$ nm. The peak at 340 nm is dominated by ACE emission, whereas the three peaks at higher wavelengths are dominated by AMMA (acceptor) emission. As the chain collapses at low pH, energy transfer between donor and acceptor occurs, causing a rise in the anthryl emission for ACE−AMMA−PMAA but little change for the ACE−PMAA.

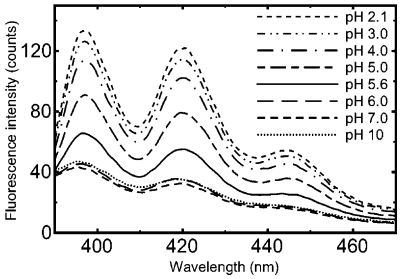

Figure 5. Data show how the AMMA emission is enhanced as the pH is lowered due to energy transfer.

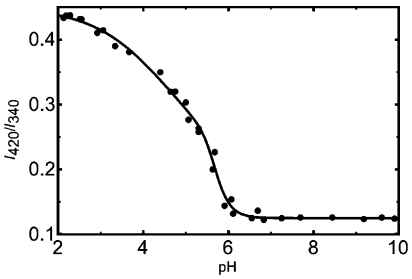

Figure 6. Ratio of emission at $\lambda_{em} = 420$ nm to emission at $\lambda_{em} = 338$ nm as a function of pH for ACE−AMMA−PMAA with excitation at 290 nm. The solid line is a fit to eq 6.

pudding" conformation, which would be expected to swell via an intermediate pearl necklace conformation. (A plum pudding model, in analogy with J. J. Thomson's model of nuclear structure, considers the collapsed PMAA as spherical, with regions more dense in PMAA connected by less collapsed segments, rather than extended as in the pearl necklace model. The pearl necklace model assumes that collapsed regions of PMAA are linked by more open, water-swollen, segments.) It is interesting to note that the lifetimes remain independent of pH up to the transition (neutralization) point, which suggests that the Coulombic repulsions between carboxylate groups can only induce macroscopic expansion of the chain above a pH of 5.7.

It is worth noting that a layered structure such as the one we describe is unlikely to be compatible with an affine swelling of the polymers. As the pH increases, the outermost parts of the chain would be expected to swell before the innermost regions, supporting, for example, previous conclusions from Raman spectroscopy experiments.[23]

Energy Transfer Measurements. For the steady-state experiments, emission spectra were recorded over a range of pH values from 2 to 10 for both the ACE−AMMA−PMAA and ACE−PMAA samples. Figure 4 shows data for the two extremes (pH 2 and pH 10) using an excitation wavelength of 290 nm. For ACE−PMAA, the spectral profile remains invariant with pH. Consequently, it can be concluded that the steady-state emission of the ACE label is insensitive to its environment. This is in agreement with previous studies in our laboratories.[19] Figure 4 reveals that for the ACE−AMMA−PMAA sample the ACE (donor) and AMMA (acceptor) emit at 340 and 430 nm, respectively. At high pH the donor emission peak at 340 nm in the ACE−AMMA−PMAA spectrum is quenched compared to the same peak in the ACE−PMAA profile. Anthryl emission is observable at ∼420 nm and is probably due to a combination of a very small amount of direct excitation at 290 nm as well as some energy transfer via the ACE donor. (We cannot preclude energy transfer in a swollen chain if donor and acceptor labels are separated by only a few monomers.) In acidic conditions fluorescence quenching of ACE occurs and emission from the AMMA chromophore increases as a result of energy transfer. The fact that enhanced energy transfer occurs at low pH in the current study is similar to that reported by Guillet et al. in their investigation[44] of a PMAA chain labeled with a naphthalene donor and an anthryl acceptor sited at the chain terminus. The authors of this earlier investigation[44] concluded that energy transfer was enhanced due to the hypercoiled conformation and also as a result of the enhanced mobility of the chain ends.

The degree of energy transfer can be estimated from

$$\frac{\text{intensity of AMMA}}{\text{intensity of ACE}} = \frac{I(\lambda_{em} = 420\text{ nm})}{I(\lambda_{em} = 340\text{ nm})} \qquad (7)$$

via steady-state spectra, using an excitation wavelength of 290 nm sampled over the entire pH range. We show in Figure 5 the increase in AMMA emission with pH. In Figure 6, we show the degree of energy transfer (eq 7) as a function of pH. The curve in Figure 6 has the same form as those observed by other authors using different chromophores attached or dispersed in polyelectrolyte systems to reveal the conformational transition.[18,34]

The ratio of the emission peaks at 420 and 340 nm, I_{420}/I_{340} (Figure 6) increases as the polymer collapses from an expanded (at high pH) to a coiled conformation (at low pH). The phenomenon is reversible, and the same data are obtained when the chain swells. Further examination of Figure 6 reveals that a gradual decrease in the intensity ratio is apparent between pH 2 and 5. This behavior contrasts with that observed when $\langle\tau\rangle$ of the ACE donor is plotted for ACE−AMMA−PMAA over a similar pH range: between pH 2 and 5 a plateau is evident (Figure 2). In order to confirm that these observations are not simply due to a pH dependence of the fluorescence from the ACE and AMMA labels themselves, we have examined the behavior of single-labeled samples: besides noting that the steady-state spectra for ACE−PMAA were invariant with pH (Figure 4), we have also performed steady-state excitation spectra on AMMA−PMAA to demonstrate that absorption at 290 nm by the AMMA does not contribute to the results presented here (see Supporting Information). UV absorption spectroscopy experiments support this point by confirming that minimal excitation of the anthryl species occurs at 290 nm.[52] We conclude, therefore, that the pH dependence of the steady-state intensity data for ACE−AMMA−PMAA at low degrees of ionization can only be explained by the occurrence of energy transfer. In addition, the nonequivalence of the $\langle\tau\rangle$ data and the

intensity ratio measurements for ACE−AMMA−PMAA at low pH infer that deactivation by additional photophysical processes to that of nonradiative energy transfer may occur in this system. This will be discussed in more detail later in this section. In the region between pH 6 and 10, I_{420}/I_{340} for ACE−AMMA−PMAA remains approximately constant, indicating no major changes in the chain conformation (Figure 6). In order to obtain the neutralization point, we fitted the data, plotted in Figure 6, to eq 6 and obtained a neutralization pH for PMAA of 5.7, in good agreement with the lifetime results. Potentiometric experiments have been performed[4] which suggest that PMAA has a broad and ill-defined neutralization region which has been attributed to a gradual breakdown in short-range interactions.[53] The energy transfer measurements described here are ideal for interrogating such phenomena because the technique is only responsive to interactions occurring at distances of a few nanometers.

When donor−acceptor pairs are randomly attached to the polymer chain, the distribution of distances between such pairs is related to the chain dimensions. Two factors affect this distribution: the concentration of donor and acceptor and the location of donor and acceptor within the chain (i.e., whether they are located at the center of a coil or at the extremities).[54] For several acceptors per chain, the probability of energy transfer in optimum conditions (low pH) increases because it is likely that one acceptor chromophore will be closer to the donor than the average distance between all the possible chromophore pairs present in the system. Steady-state data cannot be used to determine the distance distribution. Distance distributions have been expressed as Lorentzian functions,[55] but an analysis for our situation should consider the donor−acceptor distance distribution to decay exponentially with number of monomers. End-to-end distances have been calculated assuming a Gaussian distribution function to model the energy transfer efficiency.[44] All of these theoretical treatments are postulated assuming that segmental diffusion does not occur on the time scale of the energy transfer. However, no such assumption is necessary for DLS, and this is used to estimate an approximate size of the conformation adopted by PMAA in both acidic and basic conditions.

Radiative energy transfer is a two-step process involving the emission of a fluorescence photon by D and reabsorption of that photon by A as outlined below:

$$D^* \rightarrow D + h\nu_F$$

$$A + h\nu_F \rightarrow A^*$$

This mechanism does not affect the donor decay; however, the fluorescence intensity decreases with increasing [A]. The efficiency of transfer is governed by the spectral overlap between D and A and the molar extinction coefficient of the acceptor.

Nonradiative energy transfer is defined as

$$D^* + A \rightarrow D + A^*$$

This process occurs via a single step as a consequence of dipole−dipole interactions and is dependent upon the spectral overlap of D and A and the distance between the two. In contrast to the radiative process, the lifetime of D is critically dependent upon the concentration of acceptor. Consequently, lifetime data can be used to differentiate the degree of nonradiative to radiative energy transfer in a system.

When energy transfer (ET) occurs in solution, the radiative process is often dominant, and so its effects must be accounted for when studying the nonradiative component. For example, in a comprehensive energy transfer study between *p*-terphenyl and tetraphenylbutadiene in toluene solution the total energy transfer efficiency, ET was observed[56] to be the sum of the contributions from the radiative and nonradiative components,

$$ET = ET_{radiative} + ET_{nonradiative} \quad (8)$$

The contribution of each component was observed to vary with the concentration of acceptor species. In the *p*-terphenyl/tetraphenylbutadiene system at tetraphenylbutadiene concentrations less than 10^{-4} M, the radiative process is dominant while at high [A] ($\sim 10^{-2}$ M) the nonradiative mechanism prevails.

The steady-state intensity ratios shown in Figure 6 provide information about the total degree of energy transfer in this system. The lifetime data for ACE−AMMA−PMAA in Figure 2, on the other hand, report exclusively on the nonradiative process. These features from the steady-state and time-resolved experiments can be used to provide valuable short-range information regarding the mechanism of the smart response in PMAA.

Reference to Figure 6 reveals that a gradual decrease in the intensity ratio is apparent between pH values 2 and 5. Here the ratio of the radiative component to the total energy transfer decreases because the lifetime data (see Figure 2, which reports on the nonradiative component) remain constant in this pH range. In the hypercoiled conformation of ACE−AMMA−PMAA, the *local* concentration of acceptor will be high (much higher than the nominal concentration of anthryl chromophore in the solution sample, which is $\sim 10^{-6}$ M, from the labeling conditions adopted in the current study). Consequently these circumstances are conducive to promotion of a high contribution from the radiative component. (Certainly for the *p*-terphenyl/tetraphenylbutadiene system the radiative component dominates[56] between acceptor concentrations of 10^{-6} and 10^{-4} M.) For PMAA at pH 2, there are strong attractive hydrophobic forces between the backbone methyl groups, in addition to hydrogen-bonding interactions between COOH units. These have previously been referred to as short-range interactions.[56] However, as the pH is increased, an increasing concentration of carboxylate anions is present.[4] The mutually repulsive interactions between the negatively charged species serve to gradually break down the short-range hydrophobic interactions involving the methyl units. This has been suggested[56] to lead to a gradual expansion of the PMAA chain until a critical point is reached where a macroscopic transition occurs at ca. pH 6 when neutralization of the PMAA is complete. Under these conditions, repulsions between carboxylate anions dominate, the hydrophobic attractions are completely broken down, and the chain expands to a water-swollen structure. Classically, the pH-dependent behavior of PMAA has been revealed in titration plots which comprise two linear regions separated by a marked inflection.[4] These plots have been interpreted as follows: the first linear portion is associated with increasing concentrations of anions as the degree of ionization increases. The point of inflection can be attributed to a slowing down in the rate of decrease in acid strength. This has been suggested to be a consequence of a sudden uncoiling of the polymer chains increasing the separation between the remaining acid groups.

The intensity data in Figure 6 illustrate these gradual rearrangements of the polymer chain as the pH increases from 2 to 5; the *local* acceptor concentration also decreases gradually within this pH range as the short-range interactions are broken down and the chain partially expands. These energy transfer data provide strong evidence for a partial expansion (or structural rearrangement) of PMAA prior to the macroscopic switch at

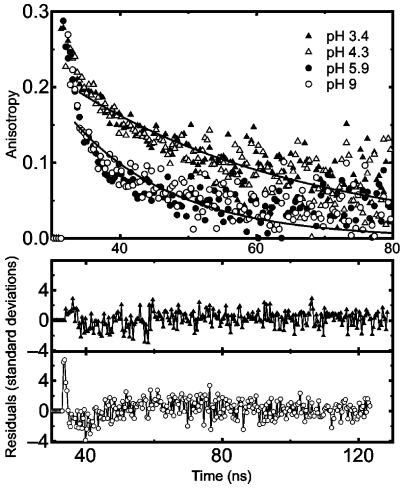

Figure 7. Anisotropy decays (top graph) for ACE−AMMA−PMAA as a function of pH (here $\lambda_{ex} = 370$ nm and $\lambda_{em} = 450$ nm). The solid lines are fits to the data for pH values of 3.4 and 9. Below, the residuals are shown for the analyses of samples at pH 3.4 and pH 9. The residuals from the analysis of the sample at pH 9 are the lower of the two. We show the residuals over the full fitting range, but the scatter in the different sets of data at longer times means that the best presentation of the anisotropy decays is limited to <80 ns. The residuals to the pH 9 data show that the single-exponential fit is limited to the "tail" of the data, as discussed in the text.

the neutralization point. In addition, and crucially, the donor−acceptor experiments have allowed the breakdown in short-range interactions to be monitored experimentally in PMAA. A similar trend in intramolecular energy transfer has been observed[44] in a double-labeled poly(*N*-isopropylacrylamide) (PNIPAM) sample; a gradual increase in the degree of energy transfer was reported well below the conformational transition temperature of PNIPAM. This was also attributed[44] to the existence of short-range interactions at temperatures below the conformational transition of the polymer, which were inferred to be a result of conformational rearrangements prior to collapse into the globular structure.

The energy transfer efficiency is a function of the distance r between the donor and acceptor

$$\mathrm{ET} = \frac{1}{1 + (r/R_0)^6} \tag{9}$$

where R_0 is the average donor−acceptor distance at which 50% energy transfer takes place.[38] The energy transfer efficiency can be calculated from

$$\mathrm{ET} = 1 - \frac{\tau_{\mathrm{ET}}}{\tau_{\mathrm{D}}} \tag{10}$$

where τ_{D} and τ_{ET} are the respective lifetimes in the absence and presence of acceptor.

We have estimated ET from eq 10 by using an average lifetime calculated from eq 2 from the donor decays of ACE−AMMA−PMAA as a function of solution pH. The nonradiative transfer efficiency remains constant between pH 2 and 5 (ET $\approx$ 0.14 in this region) and decreases between pH 5 and 6 as the coil expands: i.e., at pH 5.4 the ET drops to 0.11 and then to essentially 0 by pH 5.6. At this point, the macroscopic transition is complete, in agreement with our estimates of the neutralization point from the fits to the data shown in Figures 2 and 7.

The distance between the donor and acceptor in the hypercoiled conformation was calculated as 3.4 nm from eq 9 using $R_0 = 2.5$ nm for an anthryl and naphthyl donor/acceptor pair.[42]

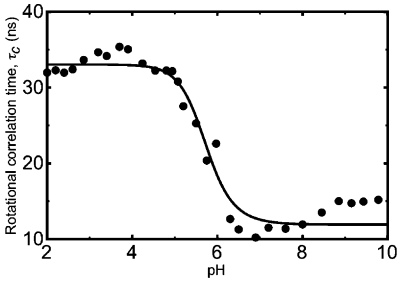

Figure 8. Rotational correlation times as a function of pH ($\lambda_{ex} = 370$ nm and $\lambda_{em} = 450$ nm). The solid line is a fit to eq 6 and reveals the neutralization point as pH 5.7.

This seems reasonable, since we estimate the total size of the hypercoil to be 8 nm from the DLS data discussed below. The coil expands to ~15 nm at pH 6, which is beyond the critical transfer distance for this system; consequently, the energy transfer efficiency decreases dramatically. This is reflected in the data shown in Figure 2; at pH values in excess of 6, the lifetime data in the presence and absence of acceptor can be superimposed.

Time-Resolved Anisotropy Measurements. For the time-resolved anisotropy experiments the anthryl label (in ACE−AMMA−PMAA) was selectively excited and analyzed. The anisotropy decays of the ACE−AMMA−PMAA sample are shown at several different pH values in Figure 7. In acidic conditions, the hypercoiled PMAA retards the decay, a situation that is reversed in basic conditions. Previous work on the aqueous solution behavior of PMAA has shown that a 1-vinylnaphthalene label can sense free rotations in the hypercoiled conformation.[35] Since the AMMA label in the current work is also capable of free rotation, we wish to concentrate on monitoring motion of the polymer backbone. We have therefore simplified our analysis by fitting the longest times of the decay (the "tail" of the data), which should reflect largely backbone motion, where a simple exponential decay (eq 4) suffices to model these data. The residuals also shown in Figure 7 clearly demonstrate that at long times a single-exponential function adequately fits the data. The quality of single-exponential analyses is very good, with all of the (normalized) χ^2 values lying between 1.0 and 1.8. These TRAMS results reveal a clear demarcation between the hypercoiled and expanded states of PMAA. In Figure 8, the rotational correlation time is plotted as a function of pH. The neutralization point was estimated at pH 5.7 by fitting these data to eq 6.

The shape of the pH dependence of the rotational correlation time (Figure 8), with a maximum at pH ~4 and a minimum at pH ~7, demands some explanation. We first consider pH ~4 where a maximum in the data occurs, as in previous observations for PMAA with different labels.[15,35] Presumably this peak in correlation time data is due to the freedom that the AMMA label has to rotate independently of the chain backbone, i.e., about an axis defined by the single bond linking the chromophore to the chain backbone. One might expect the chain to become less mobile with decreasing pH to the point at which full acidification occurs at pH ~2. As the chain collapses, however, hydrogen bonding between carboxylic groups and any remaining carboxylate ions increase the rigidity of the chain, causing an increase in the rotational correlation time. Under these conditions, AMMA, through its free rotation, monitors the microviscosity of the polymer coil. Consequently, our data suggest that since the motion is slowest at pH ~4, free rotation is hindered due to an increased microviscosity in the hypercoil (i.e., the microviscosity is maximized at this pH). Clearly this

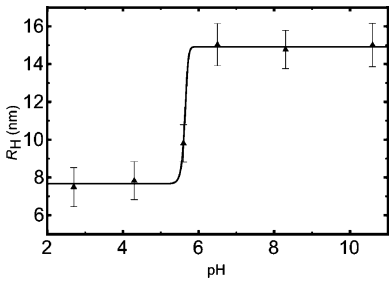

Figure 9. Hydrodynamic radii as a function of pH for (unlabeled) PMAA as measured by dynamic light scattering. The size of the polymer nearly doubles for solutions with pH greater than 5.7 (the neutralization point measured in the current work). The solid line is a best fit to eq 6.

effect diminishes when the chain is swollen: the microviscosity is at a minimum under these conditions. The effect also diminishes at very low pH (<4) when there are no (or few) remaining carboxylate ions. (The coil is presumed to partially expand under very acidic conditions.) The pH at which the rotational correlation time is a maximum is therefore between the neutralization point, and full acidification, which is pH ~4 in our data. This is in agreement with results using other dyes.[15,35] ACE, unlike AMMA, is linked to the backbone by two bonds and so is unable to move independently of the main chain. Consequently, no such maximum appears in time-resolved anisotropy data for ACE-labeled PMAA since it is unable to sense the microviscosity within the hypercoiled conformation.[35]

Another noteworthy point is the fact that TRAMS using the AMMA label is insensitive to the gradual coil expansion/rearrangement between pH values 2 and 5 as revealed by the steady-state energy transfer experiments. These rearrangements are a consequence of the breakdown of short-range (<2 nm) interactions (for example, between adjacent methyl groups or adjacent segments) which result in subtle changes in the coil structure. Energy transfer experiments are ideally placed to monitor such short-range interactions. TRAMS, on the other hand, are sensitive to the macroscopic switch in conformation since this significantly affects the mobility of the label: the coil dimensions (see DLS data below) increase dramatically at the neutralization point which consequently reduces the local microviscosity and increases the rate of motion of the AMMA label.

Finally, the increase in correlation time (see Figure 8) above pH 6 is likely to reflect shielding caused by the addition of NaOH to adjust the pH of the solution. Presumably a partial collapse occurs under these conditions due to the drive of the hydrophobic units to minimize water contacts. An increase in correlation time is consequently observed. (This hydrophobic drive to induce coil collapse has been used previously to shift the conformational transition of certain acrylic acid-based polymers to higher pH by simple copolymerization with a hydrophobic monomer such as styrene.[57]) A similar screening effect and resultant partial collapse has also, for example, been observed in the swelling of PMAA gels.[58]

Dynamic Light Scattering. Solutions of polyelectrolytes show a qualitatively different behavior compared to that of neutral polymers. With the transition from a coiled to an open chain conformation, the hydrodynamic radius R_H increases. The hydrodynamic radius cannot be treated as the exact size of the polymer because it is related to the diffusive properties of the polymer in its solvated state. For the same reason, R_H should not be compared with the subtle rearrangements in chain conformation deduced from the steady-state energy transfer measurements between pH values 2 and 5. The change in size of the chain with pH can be seen from the results shown in Figure 9, where the transition to the open coil conformation occurs at a pH of 5.7. The analysis of the light scattering data treats the polymer as a hydrodynamic sphere, and we note that in swelling the chain increases in size from $R_H = 7.7$ to 15 nm. We note that, despite the fit to the DLS data suggesting the transition is complete over a very narrow range in pH, the quantity of data does not allow us to make this conclusion. Nevertheless, intrachain rearrangements determined by lifetime and steady-state experiments occur over a considerably broader range of pH than the transition to an open coil confirmation determined by DLS.

Conclusions

A detailed study of the pH-induced conformational transition of poly(methacrylic acid) has been performed using three fluorescence techniques (energy transfer, fluorescence lifetime, and time-resolved anisotropy measurements), supported by data from dynamic light scattering. The fluorescence techniques and dynamic light scattering reveal that the transition occurs at a pH value of ~5.7, which is in agreement with numerous earlier measurements. Crucially, these techniques are also sensitive to different length scales and have provided a comprehensive picture of the conformational switch of PMAA.

Energy transfer studies (which are sensitive to the nanometer scale) reveal contributions from radiative and nonradiative processes and have provided valuable information regarding the mechanism of the smart response in PMAA. These experiments have monitored the breakdown in short-range interactions between methyl units and carboxylic acid and carboxylate anions as the pH increases toward neutralization. A gradual rearrangement of the coil results over several pH units as mutual repulsion between increasing concentrations of carboxylate anion begins to dominate. At a critical pH (as revealed by DLS in particular), repulsive interactions involving anions serve to expand the coil into a water-swollen structure breaking down any remaining hydrophobic forces of attraction in the process. The combination of data from fluorescence energy transfer, TRAMS, and DLS provide unique, conclusive evidence for local intrachain rearrangements prior to the sudden macroscopic change in conformation at the neutralization point of PMAA.

Time-resolved fluorescence measurements reveal three lifetimes for the hypercoiled structure of PMAA, which we interpret to be a result of different regions of solvent concentration within the polymer chain. This suggests that the polymer expansion is cooperative rather than affine (different parts of the polymer chain swell at different points) and is consistent with the model deduced from the energy transfer and DLS measurements described above; i.e., short-range rearrangements occur prior to the macroscopic switch in conformation.

Acknowledgment. We thank the Engineering and Physical Sciences Research Council for support (GR/R74383/01). We thank Dr Ramune Rutkaite for her help with some of the measurements and Ben Ryan for UV spectroscopy on the AMMA−PMAA.

Supporting Information Available: Steady-state excitation spectra of ACE−AMMA−PMAA and AMMA−PMAA; relaxation times from the DLS experiments at three different pH values. This material is available free of charge via the Internet at http://pubs.acs.org.

References and Notes

(1) Tripathy, S. K., Kumar, J., Nalwa, H. S., Eds. *Handbook of Polyelectrolytes and Their Applications*; American Scientific: Stevenson Ranch, CA, 2002.

(2) Takahashi, M.; Yoshikawa, K.; Vasilevskaya, V. V.; Khokhlov, A. R. *J. Phys. Chem. B* **1997**, *101*, 9396−9401.
(3) Wensel, T. G.; Meares, C. F.; Vlachy, V.; Matthew, J. B. *Proc. Natl. Acad. Sci. U.S.A.* **1986**, *83*, 3267−3271.
(4) Arnold, R. *J. Colloid Sci.* **1957**, *12*, 549−556.
(5) Barone, G.; Crescenzi, V.; Quadrifoglio, F. *Ric. Sci.* **1965**, *35*, 1069−1081.
(6) Katchalsky, A.; Spitnik, P. *J. Polym. Sci.* **1947**, *2*, 432−446.
(7) Mandel, M. *Eur. Polym. J.* **1970**, *6*, 807−822.
(8) Mandel, M.; Leyte, J. C.; Stadhouder, M. G. *J. Phys. Chem.* **1967**, *71*, 603−612.
(9) Anufrieva, E. V.; Birshtein, T. M.; Nekrasova, T. N.; Ptitsyn, C. B.; Sheveleva, T. V. *J. Polym. Sci., Part C* **1968**, *16*, 3519−3531.
(10) Eisenberg, H. *J. Polym. Sci.* **1958**, *30*, 47−66.
(11) Katchalsky, A. *J. Polym. Sci.* **1951**, *7*, 393−412.
(12) Noda, I.; Tsuge, T.; Nagasawa, M. *J. Phys. Chem.* **1970**, *74*, 710−719.
(13) Barone, G.; Crescenzi, V.; Liquori, A. M.; Quadrifoglio, F. *J. Phys. Chem.* **1967**, *71*, 2341−2345.
(14) Barone, G.; Crescenzi, V.; Pispisa, B.; Quadrifoglio, F. *J. Macromol. Chem.* **1966**, *1*, 761−771.
(15) Bednář, B.; Trněná, J.; Svoboda, P.; Vajda, Š.; Fidler, V.; Procházka, K. *Macromolecules* **1991**, *24*, 2054−2059.
(16) Chen, T. S.; Thomas, J. K. *J. Polym. Sci., Polym. Phys. Ed.* **1979**, *17*, 1103−1116.
(17) Delaire, J. A.; Rodgers, M. A. J.; Webber, S. E. *J. Phys. Chem.* **1984**, *88*, 6219−6227.
(18) Olea, A. F.; Thomas, J. K. *Macromolecules* **1989**, *22*, 1165−1169.
(19) Soutar, I.; Swanson, L. *Eur. Polym. J.* **1993**, *29*, 371−378.
(20) Crescenzi, V.; Quadrifoglio, F.; Delben, F. *J. Polym. Sci., Part A2: Polym. Phys.* **1972**, *10*, 357−368.
(21) Daoust, H.; Thanh, H. L.; Ferland, P.; St-Cyr, D. *Can. J. Chem.* **1985**, *63*, 1568−1571.
(22) Delben, F.; Crescenzi, V.; Quadrifoglio, F. *Eur. Polym. J.* **1972**, *8*, 933−935.
(23) Koenig, J. L.; Angood, A. C.; Semen, J.; Lando, J. B. *J. Am. Chem. Soc.* **1969**, *91*, 7250−7254.
(24) Heitz, C.; Rawiso, M.; François, J. *Polymer* **1999**, *40*, 1637−1650.
(25) Moan, M. *J. Appl. Crystallogr.* **1978**, *11*, 519−523.
(26) Moan, M.; Wolff, C. *Polymer* **1975**, *16*, 776−780.
(27) Moan, M.; Wolff, C.; Cotton, J.-P.; Ober, R. *J. Polym. Sci., Part C* **1977**, *61*, 1−8.
(28) Pleštil, J.; Hlavatá, D.; Labský, M.; Ostanevich, Y. M.; Bezzabotnov, V. Y. *Polymer* **1987**, *28*, 213−216.
(29) Pleštil, J.; Ostanevich, Y. M.; Bezzabotnov, V. Y.; Hlavatá, D.; Labský, M. *Polymer* **1986**, *27*, 839−842.
(30) Schwarz, G. *J. Mol. Biol.* **1965**, *11*, 64−77.
(31) Chu, D.-Y.; Thomas, J. K. *Macromolecules* **1984**, *17*, 2142−2147.
(32) Zana, R.; Lianos, P.; Lang, J. *J. Phys. Chem.* **1985**, *89*, 41−44.
(33) Jones, G., II; Rahman, M. A. *Chem. Phys. Lett.* **1992**, *200*, 241−250.
(34) Clements, J. H.; Webber, S. E. *J. Phys. Chem. B* **1999**, *103*, 9366−9377.
(35) Soutar, I.; Swanson, L. *Macromolecules* **1994**, *27*, 4304−4311.
(36) Morawetz, H. Characterization of the interpenetration of chain molecules by nonradiative energy transfer. In *Photophysical and Photochemical Tools in Polymer Science*; Winnik, M. A., Ed.; Reidel: Dordrecht, 1986; pp 547−559.
(37) Förster, T. *Faraday Discuss.* **1959**, *27*, 7−17.
(38) Lakowicz, J. R. *Principles of Fluorescence Spectroscopy*, 2nd ed.; Kluwer Academic/Plenum Publishers: New York, 1999.
(39) Förster, T. Delocalized excitation and excitation transfer. In *Modern Quantum Chemistry: Istanbul Lectures Part III: Action of Light and Organic Crystals*; Sinanoglu, O., Ed.; Academic Press: New York, 1965; pp 93−137.
(40) Liu, G.; Guillet, J. E. *Macromolecules* **1990**, *23*, 1388−1392.
(41) Liu, G.; Guillet, J. E.; Al-Takrity, E. T. B.; Jenkins, A. D.; Walton, D. R. M. *Macromolecules* **1990**, *23*, 1393−1401.
(42) Webber, S. E. *Chem. Rev.* **1990**, *90*, 1469−1482.
(43) Guillet, J. E.; Rendall, W. A. *Macromolecules* **1986**, *19*, 224−230.
(44) Liu, G.; Guillet, J. E.; Al-Takrity, E. T. B.; Jenkins, A. D.; Walton, D. R. M. *Macromolecules* **1991**, *24*, 68−74.
(45) Soutar, I.; Swanson, L.; Imhof, R. E.; Rumbles, G. *Macromolecules* **1992**, *25*, 4399−4405.
(46) Anghel, D. F.; Alderson, V.; Winnik, F. M.; Mizusaki, M.; Morishima, Y. *Polymer* **1998**, *39*, 3035−3044.
(47) Anghel, D. F.; Toca-Herrera, J. L.; Winnik, F. M.; Rettig, W.; Klitzing, R. v. *Langmuir* **2002**, *18*, 5600−5606.
(48) Amrani, F.; Hung, J. M.; Morawetz, H. *Macromolecules* **1980**, *13*, 649−653.
(49) Reed, W. F. *Macromolecules* **1994**, *27*, 873−874.
(50) Sedlák, M. *J. Chem. Phys.* **1994**, *101*, 10140−10144.
(51) Ghiggino, K. P.; Tan, K. L. In *Polymer Photophysics: Luminescence, Energy Migration and Molecular Motion in Synthetic Polymers*; Phillips, D., Ed.; Chapman and Hall: London, 1985; pp 341−375.
(52) Ruiz-Pérez, L. An experimental study of adhesion and conformational transitions in polyelectrolytes. Ph.D. Thesis, University of Sheffield, Sheffield, 2006.
(53) Leyte, J. C.; Mandel, M. *J. Polym. Sci., Part A* **1964**, *2*, 1879−1891.
(54) Yekta, A.; Winnik, M. A.; Farinha, J. P. S.; Martinho, J. M. G. *J. Phys. Chem. A* **1997**, *101*, 1787−1792.
(55) Wu, P.; Brand, L. *Biochemistry* **1994**, *33*, 10457−10462.
(56) Birks, J. B.; Kuchela, K. N. *Proc. Phys. Soc.* **1961**, *77*, 1083−1094.
(57) Ebdon, J. R.; Hunt, B. J.; Lucas, D. M.; Soutar, I.; Swanson, L.; Lane, A. R. *Can. J. Chem.* **1995**, *73*, 1982−1994.
(58) Crook, C. J.; Smith, A.; Jones, R. A. L.; Ryan, A. J. *Phys. Chem. Chem. Phys.* **2002**, *4*, 1367−1369.

MA0709957